Polymer Bulletin 30, 567–574 (1993)

Polymer Bulletin

© Springer-Verlag 1993

A nanoscopic view at the spherulitic morphology of isotactic polypropylene by atomic force microscopy

Holger Schönherr*, Daniel Snétivy, and G. Julius Vancso**

Department of Chemistry, University of Toronto, 80 St. George Street, Toronto, Ontario, Canada M5S 1A1

SUMMARY

The spherulitic morphology of isotactic polypropylene (i-PP) was investigated by a combination of optical and atomic force microscopes. Thin films of i-PP were prepared in situ by using a hot stage. The crystallization conditions were carefully selected to produce different types of spherulites including α-I, α-II, mixed, and β-III types. Atomic force microscopy (AFM) scans unveiled morphological details such as mother/daughter lamellae, cross-hatching, and thickness and orientation of the lamellae. In a few cases, macromolecules were visualized. However, due to poor resolution, only the expected chain direction within the lamellae could be determined. The advantages and disadvantages of using AFM to study the surface of spherulites is discussed.

INTRODUCTION

The recent Renaissance of structural studies of isotactic polypropylene (i-PP) ensues from the lack of a comprehensive understanding of the micro- and nanostructure of this polymer. It is known that i-PP exhibits polymorphism with at least three modifications [1-3]. However, the morphology on the micrometer scale is very complex, and some of the morphological features (for example the phenomenon of cross-hatching in the α form of i-PP) are unique [4-6]. Numerous spherulitic forms of i-PP are known and were described [7, 8, 9]. Novel morphological forms [10] have also been discovered, and it seems that the list of possible micro- and nanostructures is not yet complete. Because of the central role this polymer plays in a variety of applications, it is important that the structure be better understood. The use of $KMnO_4$ etching technique combined with electron microscopy led to the basic understanding of the principles of spherulite growth via dominant lamellae [11, 12]. Models have been postulated to explain chain packing within the lamellae of the spherulites [8], the phenomenon of cross-hatching, etc. Due to the advent of the atomic force microscopy (AFM), it is now possible to study structural details from the micrometer to the Ångstrøm scale with the same instrument [13]. AFM allows one to obtain local information about the molecular organization of bulk polymers at preselected locations of the spherulitic microstructure. Previously, it has been successfully used to investigate the nanostructure and morphology of oriented i-PP [14, 15]. In addition, lamellae of i-PP oligomers grown epitaxially on benzoic acid crystals, were studied [16]. In the present paper we focus on the use of AFM to study the details of the spherulitic morphology of this polymer.

EXPERIMENTAL PART

The samples were prepared from commercial grade i-PP (PP 8000 GK, Quantum USI, T_m = 164.9 °C DSC melt peak temperature). Films were ob-

*Current address: Institut für Organische Chemie, Johannes-Gutenberg-Universität, J. J. Becher Weg 18–20, W-6500 Mainz, Germany

**Corresponding author

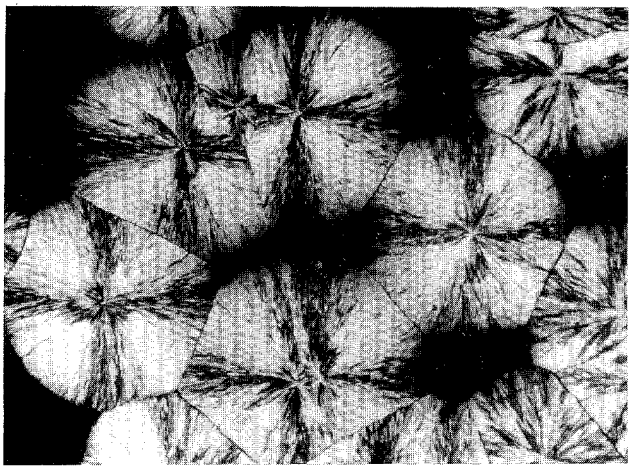

Figure 1:
α–I spherulites,
optical micrograph,
polarized light,
magnification 60 x

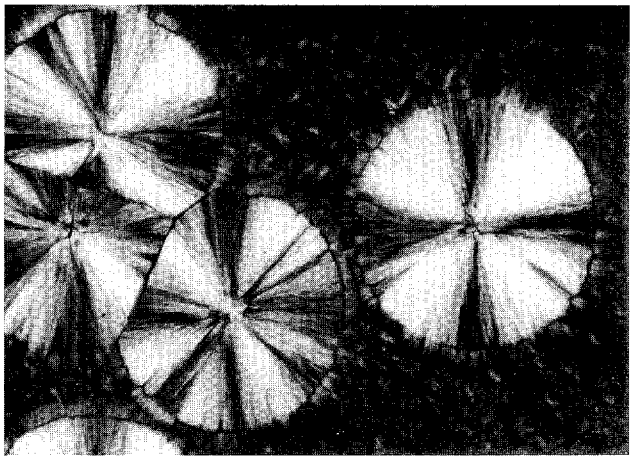

Figure 2:
α–II spherulites,
optical micrograph,
polarized light,
magnification 200 x

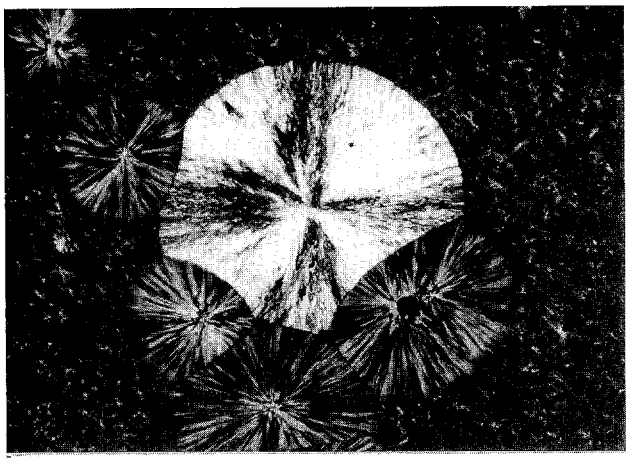

Figure 3 :
β-III spherulite
surrounded by
α-m spherulites,
optical micrograph ,
polarized light,
magnification 120 x

tained by compression moulding at 215 °C by applying a pressure of 17 metric tons for 15 minutes. Specimens with approximate thickness of 20 μm were subsequently melted and crystallized in a Mettler hot stage under N_2 flow. The temperature program used allowed the control of the nucleation density for different crystallization temperatures ranging from 110 °C to 150 °C [11]. The samples were heated with a rate of 10 °C/min from 120 to 150 °C and with 2 °C/min from 150 °C to T_{max}. The maximum temperature T_{max} was in the range between 173.0-178.0 °C. After reaching T_{max} and melting, the temperature was lowered to the crystallization temperature, as fast as the hot stage allowed. A number of samples were crystallized to completion isothermally, while others were quenched to room temperature while crystallization was still in progress. The latter method yielded good contrast between nearly mature spherulites and the matrix of rapidly crystallized polymer (fig. 1-3). The crystalline morphology of several samples was exposed by $KMnO_4$ etching, which removed superimposed amorphous material [8, 11]. The i-PP films were investigated by an Olympus BHSM optical polarizing microscope supplied by Nomarski interference contrast optics. The AFM setup was a NanoScope II system (Digital Instr.). For imaging at the micrometer level a D-, and at the nanometer level; an A-head were utilized with square-pyramidal NanoTips and Ultralevers (Park Scientific Instr.). In contrast to NanoTips (1:1), the Ultralevers have an aspect ratio of 3: 1, which should allow better imaging of steep sidewall features and deep trenches on the sample surface.

OBSERVATIONS AND DISCUSSION

The growth of spherulites was monitored by using the optical microscope, utilizing a λ/4 plate and nearly crossed polarizers. The geometric shape of the growing objects in early stages was either nearly square-like, ("quadrites") [4, 11, 12], or oval-elongated [17]. Viewed in polarized light after the completion of crystallization, the spherulites showed their typical characteristics. Depending on the crystallization conditions, various types of spherulites were obtained. For the distinction of the different types, the nomenclature introduced by Padden and Keith was used [7]. The different spherulites observed included the α-I type (fig. 1, positive birefringence, T_c= 120 °C), the α-II type (fig. 2, negative birefringence, T_c = 140 °C), various forms of mixed type spherulites α-m (fig. 3, T_c = 120 °C, no maltese cross in the polarized optical micrographs), and, sporadically, the highly negative birefringent β-III type (fig. 3, surrounded by α-m). The β-IV type spherulite [7,8] was not observed. The surfaces of the α- and β-modifications differ significantly in their textures. Under the optical microscope, the α-form (fig. 5) showed features resembling radiating bundles of lamellae. AFM images unveiled dominant lamellae with crystallographic as well as non-crystallographic branches. Crystallographic branches produced "cross-hatching" at an angle of 80°. In figures 11-15, the daughter lamellae filled the regions between the dominant lamellae. Non-crystallographic branching resulted in spherical objects. The β-modification showed a "curly" surface texture and no sign of cross-hatching (fig. 4, 6). Lamellar branching frequently occurred under small angles (20°-25°) (fig. 10). The principal direction of growth [8], as well as the filling of the enclosed space ("Popoff's leaves" [18]) were unveiled. Figures 8 and 9 show the effect of quenching on the crystallizing melt. The spherulite shown in fig. 8 was obtained in rapid crystallization (quenching to RT), whereas fig. 9 shows an isothermally crystallized α-II type (T_c = 145 °C).

The phenomenon of cross-hatching (an example for homoepitaxy), is observed in all the α-type spherulites. This was expected since in each case crystallization was performed below the critical temperature, characteristic for the upper limit of cross-hatching [11]. The AFM image shown in fig. 11 clearly shows

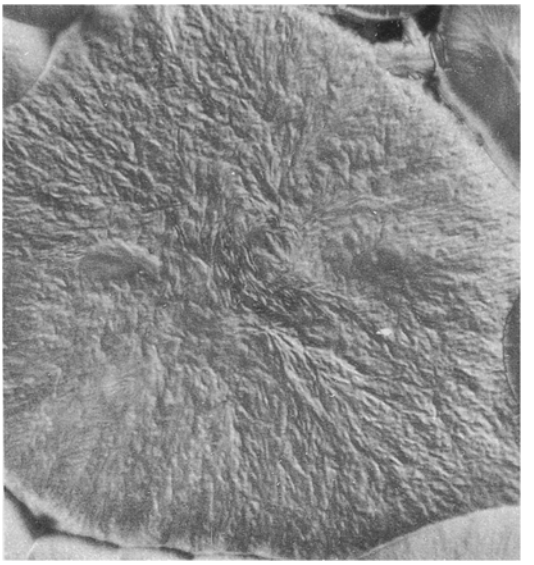

Figure 4:
β-III spherulite, optical micrograph, Nomarski interference contrast, magnification 500 x

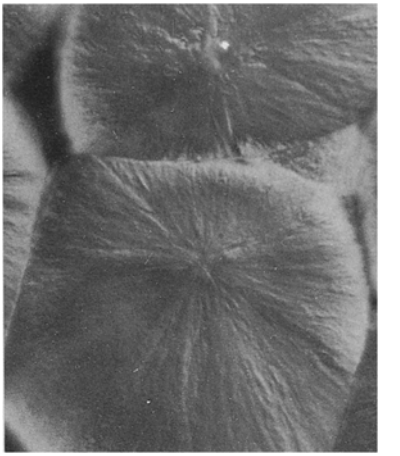

Figure 5:
α-I spherulite, optical micrograph, Nomarski interference contrast, magnification 500 x

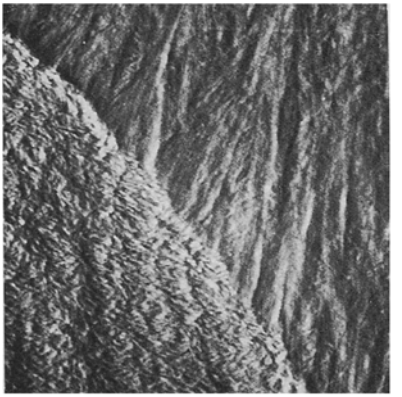

Figure 6:
Boundary region between β (left) and α (right) spherulites, T_c=110 °C, AFM scan, 15 μm x 15 μm force mode, NanoTip

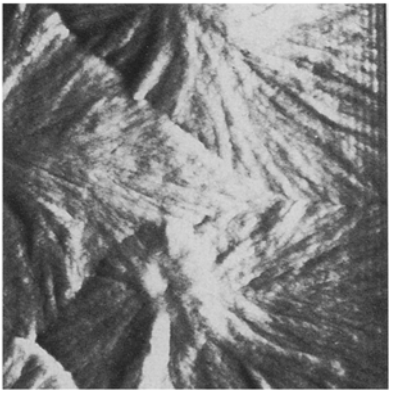

Figure 7:
α-m spherulites, quenched, AFM scan, 15 μm x 15 μm, force mode, Ultralever

crystallographic branching. Whereas these images were taken in the "height mode" (see [13] or [19]), fig. 12 shows a micrograph of a densely cross-hatched region captured in the "force mode". Unless explicitly mentioned, all the AFM scans in this study were taken in the height mode. While the z-scale does not provide accurate information about the height, the angles can nevertheless be measured, and are in the range of 80° ± 3°. Furthermore, we can conclude that except for local deviations (fig. 14), the radial lamellae are generally thicker than the tangential ones (fig. 13). Thus, AFM offers the possibility to obtain a "real space" image of these regions which resemble a 3-dimensional network, and shows single lamella in numerous epitaxial relations with other lamellae. The overall number of crystallographic branches is increasing with decreasing T_c.

Furthermore, quantitative evaluation of lamellar thickness was attempted. Unfortunately, due to difficulties with the AFM in measuring the exact shape of objects in a size similar to that of the tip, we could obtain only a qualitative or semi-quantitative result. Nearly all features observed by the AFM possess more or less rounded edges. The real shape of these objects, however, is uncertain (tip imaging). The thickness of the "lamellar" features was measured by utilizing cross-sectional plots in preselected directions. The numerical values are based on estimates made at the half-height of the lamella. Table 1 compares the average values of the lamellar thickness for different crystallization temperatures for α spherulites with values published in the literature [8, 20, 21] . The results are in good agreement. There is a clear trend present of lamellar thicknesses d as a function of T_c. An estimation of the thickness distribution is shown in figure 19. Edge-on view of the lamellae was assumed throughout this analysis [8].

Figure 15 shows two tangential lamellae in very high magnification, (d=130 Å) image size: 200 nm x 200 nm. Details of structural features at this and smaller scan sizes are very difficult to identify and interpret. The roughness of the sample surface usually limits the resolution to scan sizes of about 400 nm. Figs. 16 to 18 show stacked lamellae, in edge-on view. Fig. 17 represents an example of the interior of a film. For the sample imaged in this case, the surface of the sample (including the thinner daughter lamellae) was removed by $KMnO_4$ etching. We also tried to obtain atomic resolution on edge-on lamellae using the A-scanner. The images obtained were noisy, and allowed us to make only a qualitative conclusion. The orientation of the chains was, as expected, nearly perpendicular to the edge of the lamellae, and the values of chain packing were in the range of the a-repeat unit of the unit cell of the α-modification (6.66 Å). The quality of the AFM nanographs with molecular resolution is much poorer than those observed on extended chain crystals of oriented i-PP [14, 15].

In conclusion, AFM studies of various i-PP spherulites on the micrometer scale yielded images which reproduce the known structural features. Furthermore, molecular scale images unveiled the chain direction in the mother lamellae. It seems that in the range between typically 10 to 200 nm the applicability of AFM is hampered by tip effects, which are related to the curvature of the apex. Imaging of steep sidewall features and deep objects at the sample surface are difficult or impossible. On the other hand, AFM yields a variety of very different information about the structure which is impossible to obtain by any other single experimental technique. In addition to micromorphology, AFM reveals the orientation, thickness and thickness distribution of the lamellae, and, as it is capable of molecular imaging, chain packing distances at the sample surface, etc. AFM, although still in its infancy, has been successful in tackling a large number of different structural problems. It is to be expected that with the im-

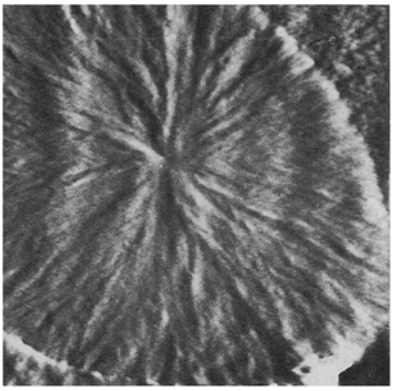

Figure 8: α-m spherulite, AFM scan, force mode, 15 μm x 15 μm, NanoTip

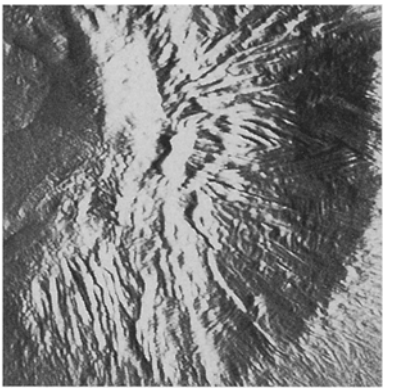

Figure 9: α-II spherulite, AFM scan, force mode, 15 μm x 15 μm, Ultralever

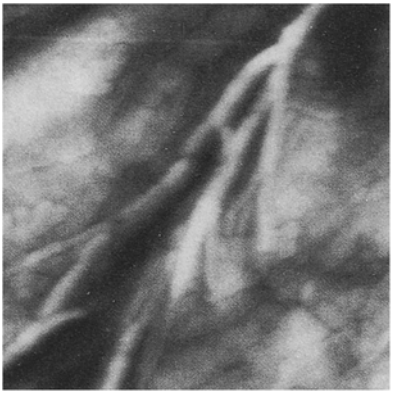

Figure 10: Non-crystallographic branching in β spherulite, T_c=110 °C, AFM scan, 2.5 μm x 2.5 μm, NanoTip

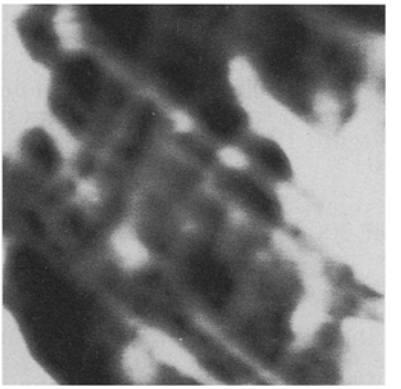

Figure 11: Cross-hatching in α-II spherulite, T_c=145 °C, AFM scan, 1.5 μm x 1.5 μm, Ultralever

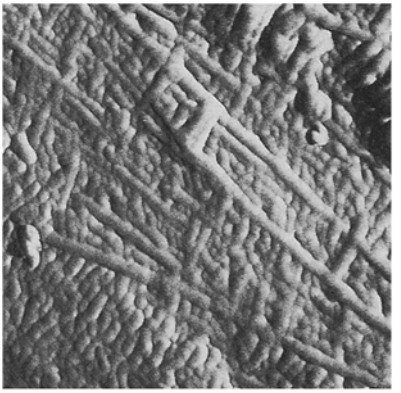

Figure 12: Cross-hatching in α-m spherulite, T_c=110 °C, AFM scan, 1.0 μm x 1.0 μm, force mode, NanoTip

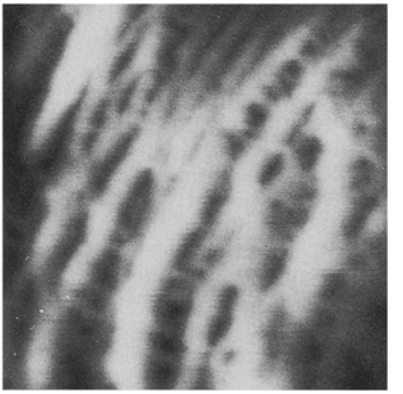

Figure 13: Mother and daughter lamellae of α-II spherulite, T_c=145 °C, AFM scan, 15 μm x 15 μm, Ultralever

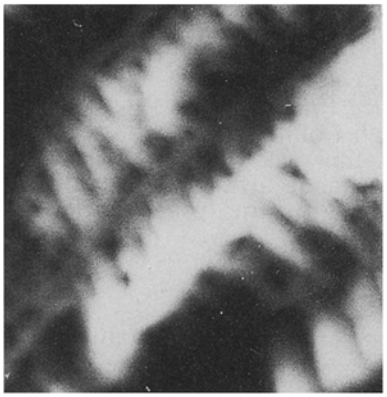

Figure 14: Thick daugthter lamellae of α-II spherulite, T_c=145 °C, AFM scan, 15 μm x 15 μm, Ultralever

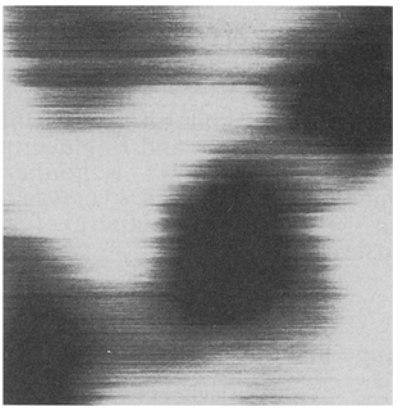

Figure 15: Tangential lamellae of α–II spherulite, T_c=145 °C, AFM scan, 200 nm x 200 nm, Ultralever

Figure 16: Stacked radial lamellae of α-I spherulite, T_c=125 °C, AFM scan, 300 nm x 300 nm, Ultralever

Figure 17: Stacked radial lamellae of α-m spherulite, T_c=125 °C, AFM scan, 250 nm x 250 nm, NanoTip

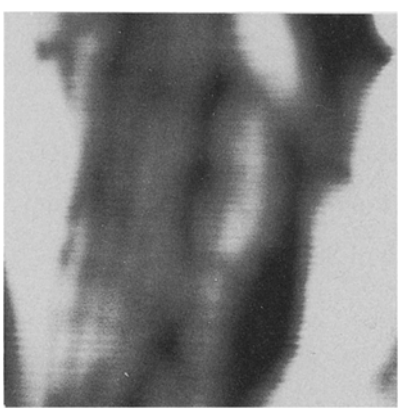

Figure 18: Stacked radial lamellae of α-II spherulite, T_c=145 °C, AFM scan, 400 nm x 400 nm, NanoTip

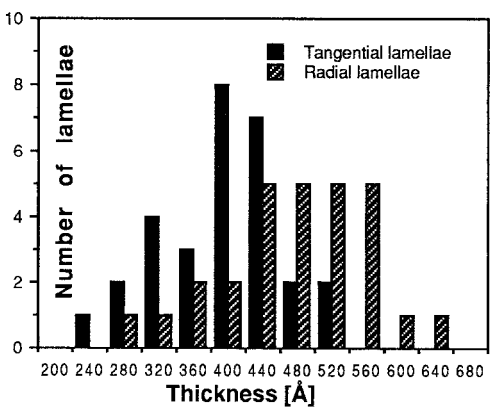

Figure 19: Distribution of the lamellar thickness for α-II spherulites, T_c=145 °C, AFM data

provement of the technique it will be capable of solving the open problems related to the self organization of macromolecules in the solid state.

ACKNOWLEDGEMENT

The authors are grateful to the Ontario Centre for Materials Research and to the Natural Sciences and Engineering Research Council of Canada for financial support. One of us (H. Schönherr) thanks the "Deutscher Akademischer Austauschdienst" for an overseas student exchange award. We would like to thank Ms. Anne Klemperer for her help with the preparation of the manuscript.

Table 1

Average lamellar thickness as a function of crystallization temperature

T_c	thickness AFM (Å)	lamellar direction	thickness literature (Å)	ref.
110 °C	100	radial	-	-
120 °C	-	-	100-130	[21]
125 °C	145	radial	140	[20]
130 °C	180	radial	140-165	[21]
145 °C	460	radial	≈ 500	[1]
145 °C	390	tangential	≈ 400	[1]

REFERENCES

1. Natta G, Corradini P, Cesari M (1956) Rend.Atti Acc.Naz.Lincei 21: 365
2. Keith HD, Padden FJ, Walter NH, Wyckoff HW (1959) Appl Phys 30: 1485
3. Turner-Jones A, Aizlewood JM, Beckett DR (1964) Makromol Chem 75:134
4. Khoury F (1966) J Res Natl Bureau Std 70A: 29
5. Padden FJ, Keith HD (1966) J Appl Phys 37: 4013
6. Lotz B, Wittmann JC (1986) Polym Sci, Part B: Polym Phys 24: 1541
7. Padden FJ, Keith HD (1959) J Appl Phy 30: 1479
8. Norton DR, Keller A (1985) Polymer 26: 704
9. Varga J (1992) J Mat Sci 27: 2557
10. Awaya H (1988) Polymer 29: 591
11. Bassett DC, Olley RH (1984) Polymer 25: 935
12. Olley RH, Bassett DC (1989) Polymer 30: 399
13. Sarid D (1991) Scanning Force Microscopy, with Applications to Electric, Magnetic and Atomic Forces. Oxford University Press, Oxford
14. Snétivy D, Vancso GJ Polymer, submitted
15. Snétivy D, Guillet JE, Vancso GJ (1993) Polymer 34: 429
16. Lotz B, Wittmann JC, Stocker W, Magonow S, Cantow H-J (1991) Polymer Bulletin 26: 109
17. Binsbergen FL, De Lange BGM (1968) Polymer 9: 23
18. Keller A (1958) in : Growth and Perfection of Crystals (Doremus RH, Roberts BW, Turnbull D (eds)). Wiley, New York 499-532
19. Magonov S, Cantow H-J (1992) J Appl Polym Sci, Appl Polym Symp 51: 3
20. Wlochowicz A, Eder M (1984) Polymer 25: 1268
21. Ceres BV, Schultz JM (1984) J Appl Polym Sci 29: 4183

Accepted March 15, 1993 K